Quantitative visualization of DNA G-quadruplex structures in human cells

Giulia Biffi[1], David Tannahill[1], John McCafferty[2] & Shankar Balasubramanian[1,3] *

[1]Cancer Research UK Cambridge Institute, Li Ka Shing Centre, Robinson way, Cambridge, CB2 0RE, UK.
[2]Department of Biochemistry, University of Cambridge, Tennis Court Road, Cambridge CB2 1QW, UK.
[3]Department of Chemistry, University of Cambridge, Lensfield Road, Cambridge, CB2 1EW, UK.

E-mail: sb10031@cam.ac.uk

SUPPLEMENTARY INFORMATION for an Article to *Nature Chemistry*

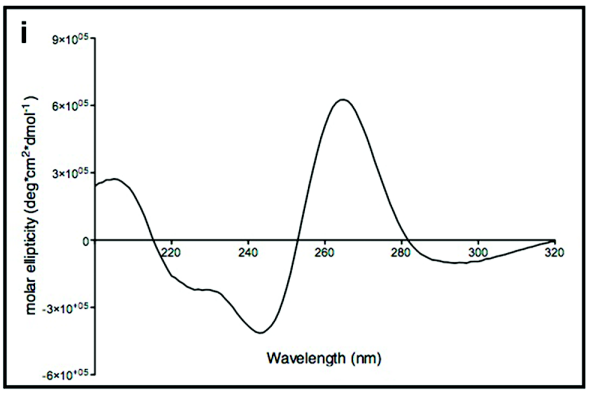
i
molar ellipticity (deg*cm2*dmol-1)
Wavelength (nm)

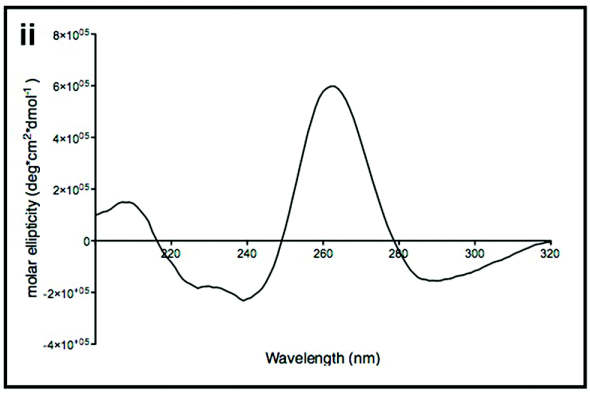
ii
molar ellipticity (deg*cm2*dmol-1)
Wavelength (nm)

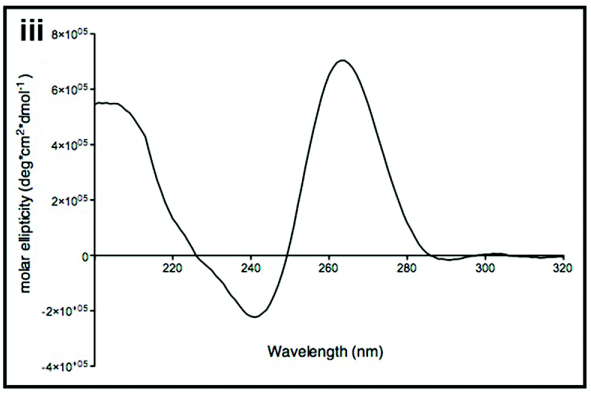
iii
molar ellipticity (deg*cm2*dmol-1)
Wavelength (nm)

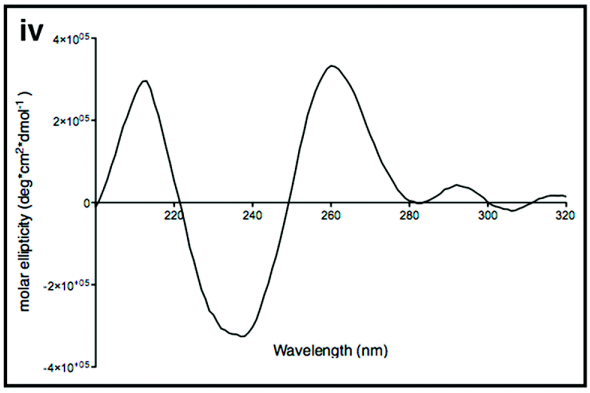
iv
molar ellipticity (deg*cm2*dmol-1)
Wavelength (nm)

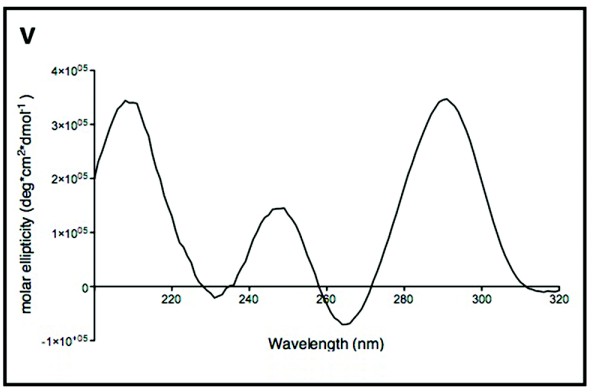
v
molar ellipticity (deg*cm2*dmol-1)
Wavelength (nm)

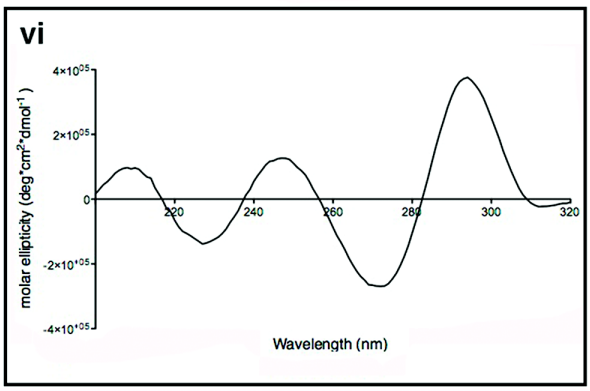
vi
molar ellipticity (deg*cm2*dmol-1)
Wavelength (nm)

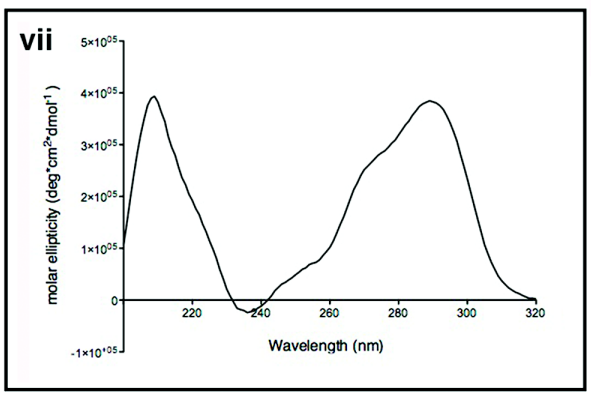
vii
molar ellipticity (deg*cm2*dmol-1)
Wavelength (nm)

Supplementary Figure 1. Biophysical analysis of G-quadruplex oligonucleotides by circular dichroism (CD) spectroscopy. CD spectra for MYC **(i)**, KIT1 **(ii)**, KIT2 **(iii)**, intermolec hTELO **(iv)**, SPB1 **(v)**, TBA **(vi)** and hTELO **(vii)** G-quadruplex structures in the presence of 100 mM KCl. The MYC, KIT1, KIT2 and intermolec hTELO spectra are characteristic of parallel G-quadruplexes with a positive peak at ~260 nm and a negative peak at ~240 nm. The SPB1 and TBA spectra are characteristic of anti-parallel G-quadruplex structures with positive peaks at ~250 nm and ~290 nm and the absence of a positive peak at ~260 nm. The hTELO spectrum is characteristic of a mixed-type propeller G-quadruplex structure.

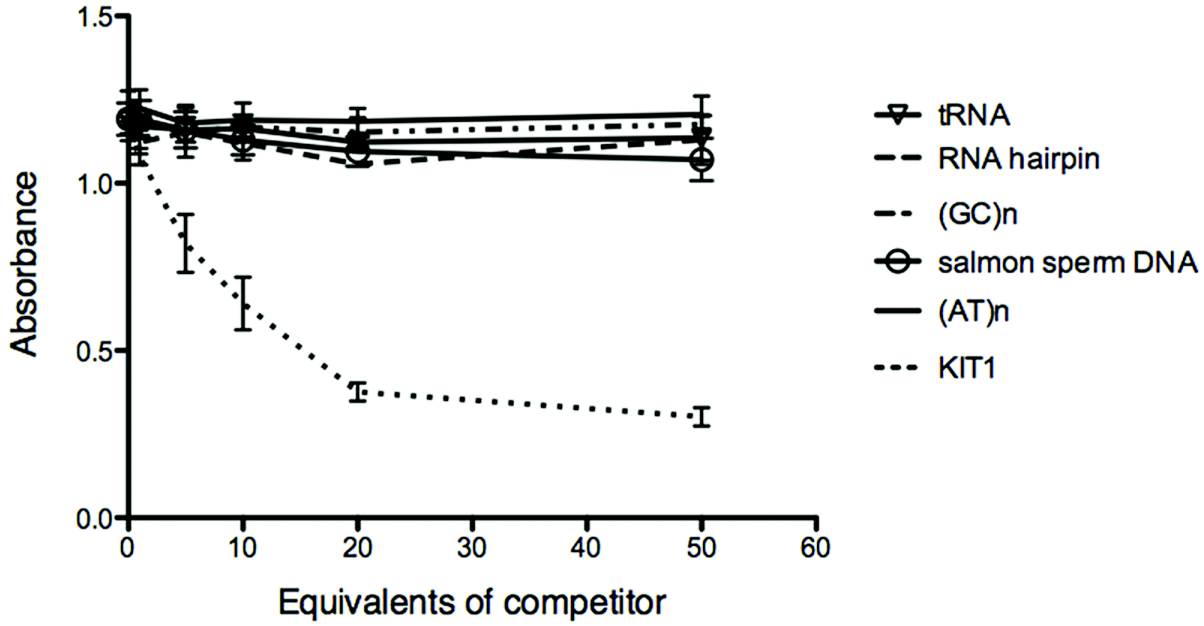

Supplementary Figure 2. Further characterization of BG4 specificity for G-quadruplex structures. Further tests of BG4 specificity were performed by competition for MYC G-quadruplex binding in ELISA experiments. BG4 was pre-incubated with 0, 1, 5, 10, 20, 50 equivalents of either KIT1 (G-quadruplex), a RNA hairpin oligonucleotide, yeast tRNA, sonicated double-stranded salmon sperm DNA, double-stranded poly$(GC)_n$ or poly$(AT)_n$ before assessment of MYC G-quadruplex binding. Competition was only achieved using the positive control KIT1 G-quadruplex oligonucleotide. Error bars represent the standard error of the mean calculated from 3 replicates.

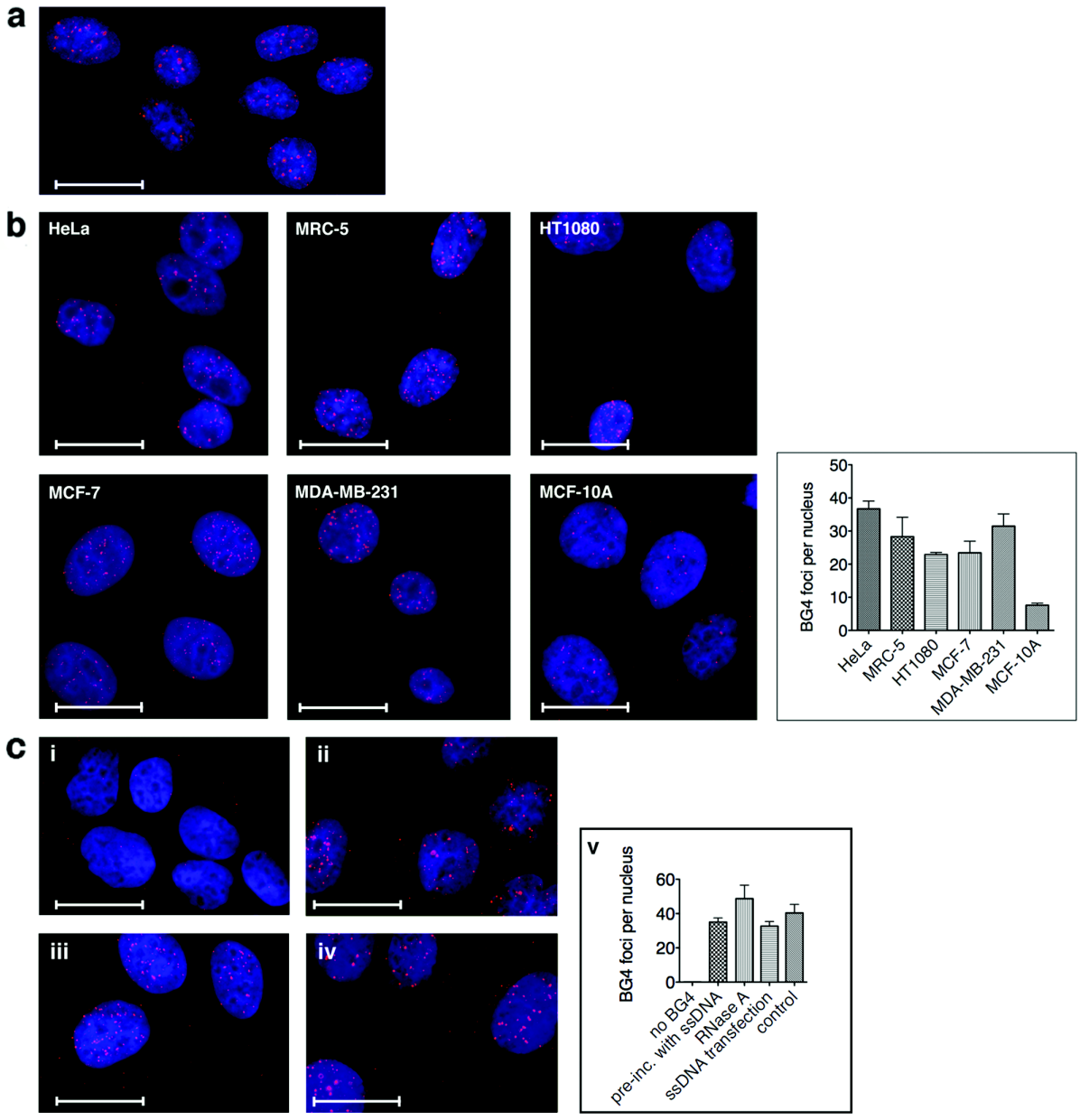

Supplementary Figure 3. Visualization of DNA G-quadruplex structures in human cells. a, Immunofluorescence showing BG4 foci (red) in U2OS cells after fixation with methanol/acetic acid. Scale bar corresponds to 20 μm. **b**, Immunofluorescence showing BG4 foci (red) in the nuclei of a panel of different human cell lines. The graph shows the quantification of BG4 foci number per nucleus. 100 nuclei were counted per cell line and the standard error of the mean calculated from a set of 3 replicates. Nuclei are counterstained with DAPI (blue). Scale bars correspond to 20 μm. **c**, Immunofluorescence for BG4 (red foci) on U2OS nuclei under different conditions. No primary antibody **(i)**. After pre-incubation of BG4 antibody with single-stranded DNA oligonucleotides **(ii)**.

Following RNase A treatment **(iii)**. After transfection with single-stranded DNA oligonucleotides **(iv)**. The graph shows the quantification of BG4 foci number per nucleus for **(i-iv)** and a control **(v)**. 100-200 nuclei were counted per condition and the standard error of the mean calculated from a set of 3 replicates. Nuclei are counterstained with DAPI (blue), scale bars correspond to 20 μm. These control experiments support the targeting and visualization of DNA G-quadruplex structures in human cells by BG4.

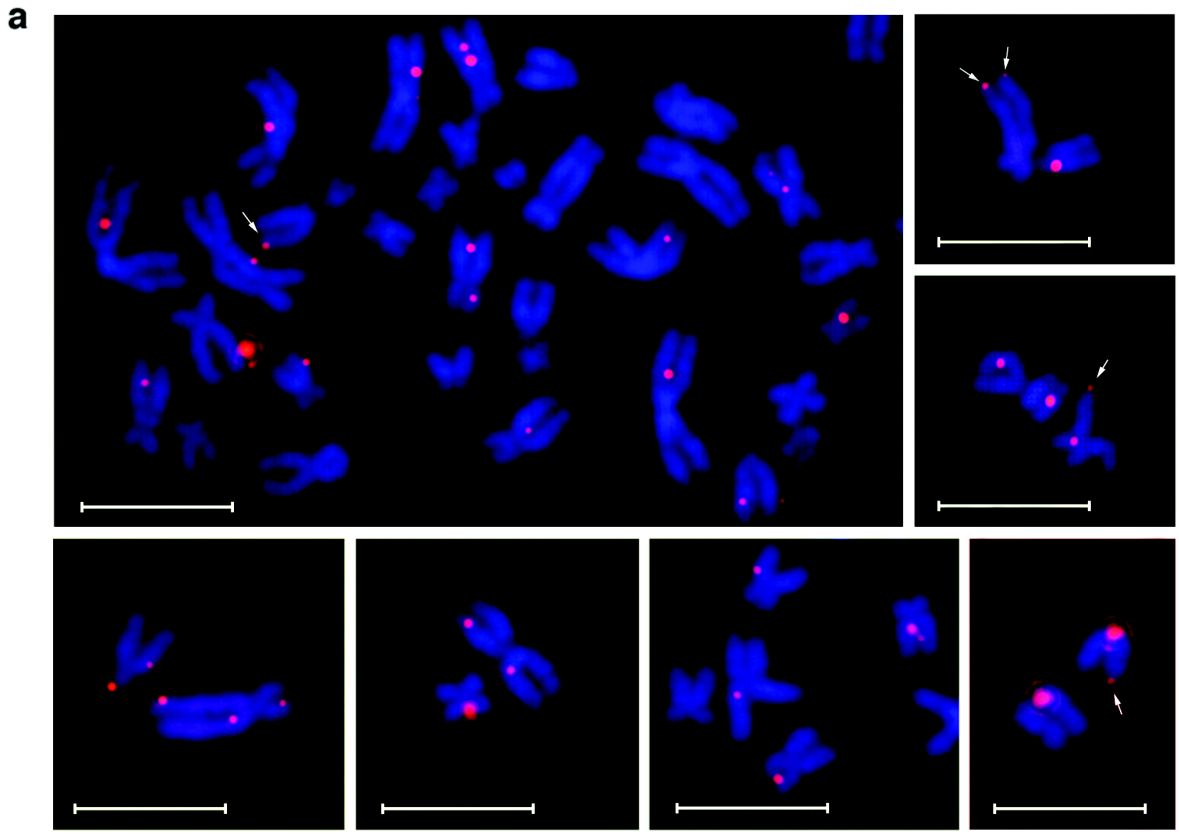
a

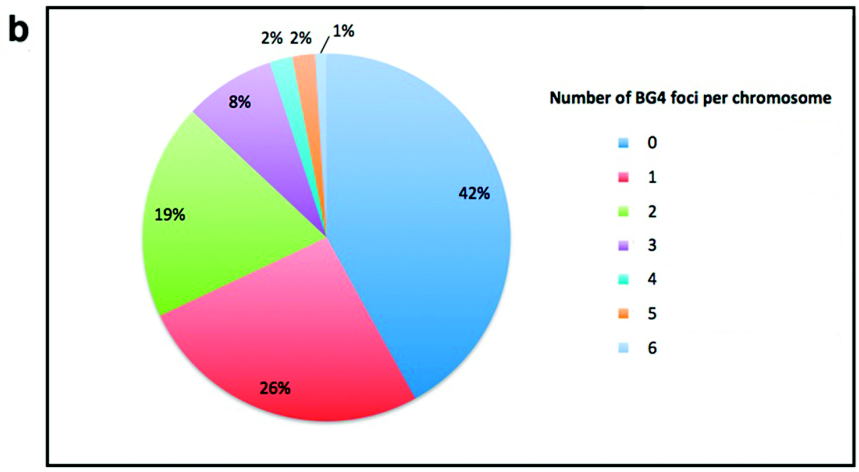
b
2%
2%
1%
8%
19%
42%
26%
Number of BG4 foci per chromosome
0
1
2
3
4
5
6

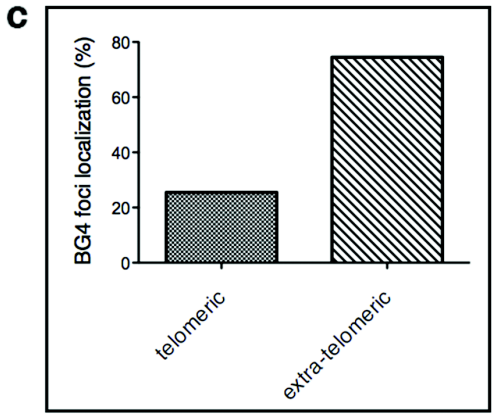
c
BG4 foci localization (%)
80
60
40
20
0
telomeric
extra-telomeric

Supplementary Figure 4. Visualization of G-quadruplex structures on human metaphase chromosomes. a, Immunofluorescence for BG4 (red foci) on metaphase chromosomes prepared from HeLa cells. The large panel shows a general view of a metaphase spread, while the smaller panels show additional representative chromosomes. Arrows indicate examples of BG4 foci localized at chromosome ends. Chromosomes are counterstained with DAPI (blue). Scale bars correspond to 5 μm. **b**, The chart represents the analysis of 100 metaphase chromosomes for BG4 foci number per chromosome and shows that the majority of chromosomes has at least one site of BG4 staining and around a third displays multiple foci. **c**, The graph represents the telomeric or extra-telomeric distribution for 100 metaphase chromosomes and clearly shows that the majority of foci lay outside the telomere.

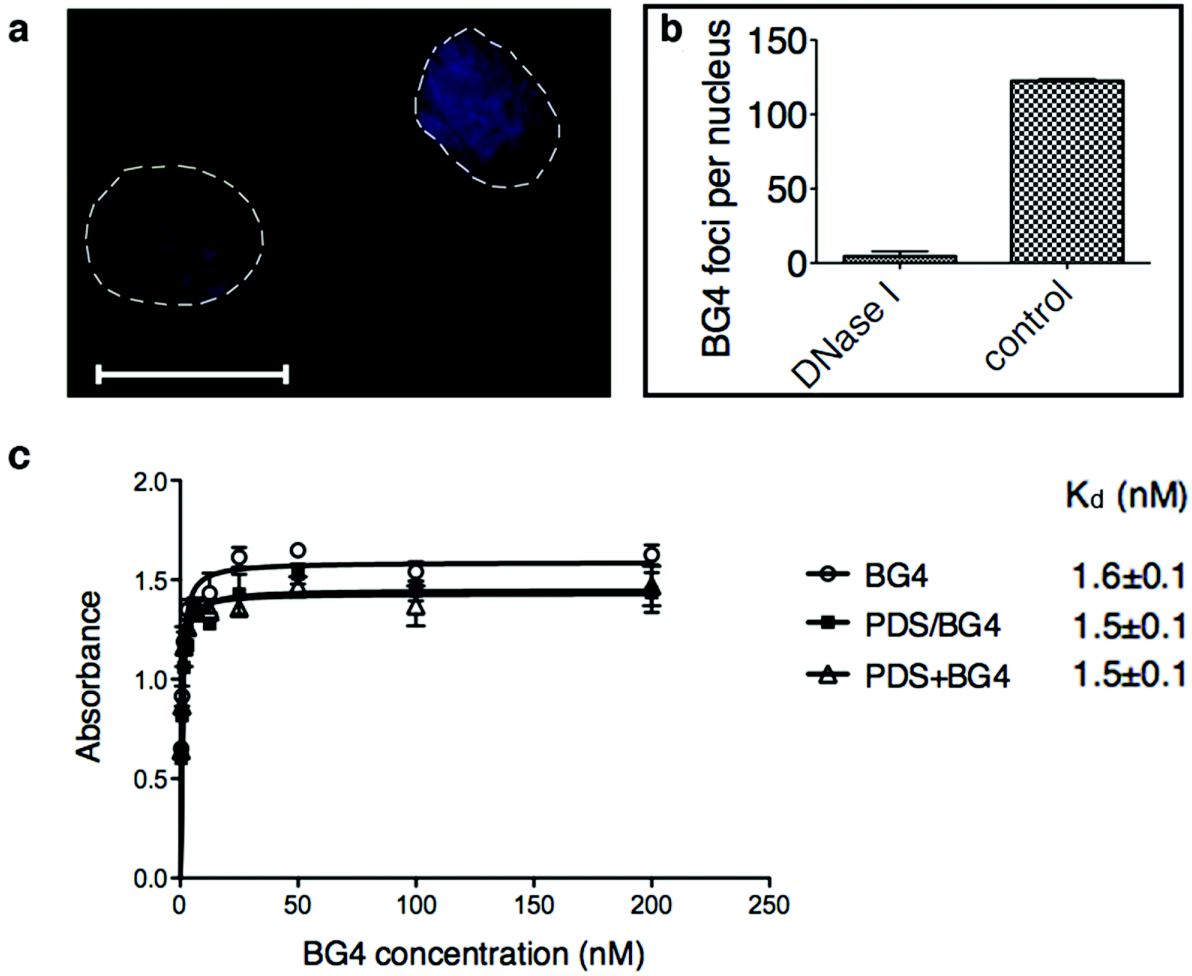

Supplementary Figure 5. Stabilization of endogenous DNA G-quadruplex structures by pyridostatin. a, Loss of BG4 staining in pyridostatin-treated cells following DNase treatment. Nuclei are counterstained with DAPI (blue), scale bar corresponds to 20 μm. The dotted lines indicate nuclei boundaries. **b**, Quantification of BG4 foci number per nucleus with or without DNase digestion after pyridostatin treatment. 100 nuclei were counted and the standard error of the mean calculated from a set of 3 replicates. **c**, Binding curves as determined by ELISA showing that BG4 affinity for the telomeric DNA G-quadruplex hTELO is not affected by either prior incubation with pyridostatin before BG4 addition (PDS/BG4) or simultaneous addition of pyridostatin and BG4 (PDS+BG4). Dissociation constants (K_d) are indicated. The standard error of the mean was calculated from 3 replicates.